

Deep blue light-emitting polymers with fluorinated backbone for enhanced color purity and efficiency

Ting Zhang^a, Renjie Wang^a, Huicai Ren^b, Zhiguang Chen^b, Jiuyan Li^{a,*}

^aState Key Laboratory of Fine Chemicals, School of Chemical Engineering, Dalian University of Technology, 2 Linggong Road, Dalian 116024, China

^bSchool of Chemistry, Dalian University of Technology, 2 Linggong Road, Dalian 116024, China

ARTICLE INFO

Article history:

Received 10 November 2011

Received in revised form

18 January 2012

Accepted 5 February 2012

Available online 9 February 2012

Keywords:

Fluorene

p-Difluorophenylene comonomer

Organic light-emitting diodes

ABSTRACT

Two fluorene-based copolymers (**PF-33F** and **PF-50F**) with *p*-difluorophenylene units in the backbone were synthesized. In comparison with the reference poly(9,9-dioctylfluorene) (**PFO**), the introduction of *p*-difluorophenylene units not only increased the fluorescent quantum yields, but also improved the spectra purity and stability of these deep blue emitting copolymers. The famous green emission band at 520 nm from fluorenone defects was never detected for these copolymers even after they were thermal annealed in air at 150 °C. Organic light-emitting diodes were fabricated using them as emitting layer and pure blue electroluminescence was obtained. It was observed that **PF-33F** based device exhibited much higher current density and brightness than **PF-50F** and **PFO** devices. A maximum external quantum efficiency of 1.14% (1.14 cd A⁻¹) and the CIE (0.16, 0.13) were achieved for **PF-33F** device, which are among the best performance for polyfluorenes reported so far.

© 2012 Elsevier Ltd. All rights reserved.

1. Introduction

Polyfluorene (**PF**)-type polymers have been established as most promising blue light-emitting materials for application in organic light-emitting diodes (OLEDs). They possess many merits such as high fluorescent quantum yields, easy syntheses and structure modification, good solubility in common organic solvents and acceptable charge mobility [1–3]. However, an undesired low-energy “green” band covering a broad spectral range from 500 to 600 nm is frequently generated in both photoluminescence (PL) and electroluminescence (EL) of **PFs** during operation, which not only damages the blue color purity and stability but also limits the emission efficiency [4].

After the intensive debate in the last few years on the origin of this long-range emission [5,6], it is more acceptable that it stems from the emissive keto defects of **PFs** (i.e. fluorenone), which are generated by chemical oxidation of the monoalkylfluorene impurities at the 9-position carbon during polymer preparation or operation in air for a long time [7,8]. Accordingly, ingenious synthetic methods were used to prepare polyfluorenes without monoalkylfluorene defects [9] and some attempts were also taken to remove the generated impurities [10]. Furthermore, various approaches have also been exploited to increase the anti-oxidation

ability of the 9-position carbon in fluorene moieties and thus to suppress the green emission. One example was to construct a rigid backbone in the fluorene moieties to inhibit the oxidation of the 9-position carbon since the oxidation of the 9-position carbon involves hybrid state conversion from sp³ to sp² and thus the change of bond angles. In this way Park et al. developed a stable blue emitting **PF** derivative with an EL efficiency of 0.7 cd A⁻¹ and CIE coordinates of (0.17, 0.12) [11]. Another attempt was to incorporate electron-deficient groups as the endcappers [12] or side-chains [13,14] of the fluorene-based polymers. Chen and coworkers have achieved high stability and improved purity in blue emission as well as improved device efficiency via capping polydioctylfluorene (PFO) chain ends with electron-deficient moieties such as oxadiazole and triazole, which can induce a minor amount of long conjugating length species (regarded as β phase) to control extents of energy transfer from amorphous matrix to the β phase [12]. In our previous report [13], the fluorene copolymers with di(tert-butyl)phenoxy)sulfonyl-phenylene comonomer showed stable blue PL even after thermal annealing in air and pure blue EL. The improved spectral stability of these **PFs** was suggested to benefit from the strong electron-withdrawing nature of the sulphonate side groups that facilitated the anti-oxidation ability. However, the introduction of these sidechain groups also resulted in the decrease in the charge mobility and the fluorescent quantum yields of the copolymers. Similarly, the strong electron-deficient 2,8-dihexyldibenzothiophene-*S,S*-dioxide-3,7-diyl units was also used as the building block to synthesize pure blue light-emitting **PF**

* Corresponding author. Fax: +86 411 84986233.

E-mail address: jiuyanli@dlut.edu.cn (J. Li).

derivatives. However, an EL efficiency of those polymers was only 0.24 cd A^{-1} with a blue color of (0.18, 0.15) [15].

Apparently, the type of the functional comonomer and its content ratio in polymers are two important factors to determine both the luminescent and charge-transporting properties and thus the EL performance of these polymers. The functional groups should be properly selected and their ratio should be well tuned so that the blue color purity and stability can be improved without expense of luminescent quantum yield and charge mobility. In this paper, we reported the synthesis and properties of two novel fluorene-based copolymers containing *p*-difluorophenylene comonomer, **PF-33F** and **PF-50F** (Scheme 1). The *p*-difluorophenylene group was selected as an important building block with the expectation to tune the electronic state of the polymer backbone and to improve spectral purity and stability of the polymers [16,17]. For optimization purpose, the content ratio of the *p*-difluorophenylene unit was varied from 33 mol% (**PF-33F**) to 50 mol% (**PF-50F**). For comparison, poly(9,9-dioctylfluorene) (**PFO**), was also synthesized and studied under the same conditions. The PL spectral stability of these polymers was investigated by monitoring the emission spectra before and after thermal annealing in air. These polymers were also used as emitting layer to fabricate OLEDs. The results show that, both the PL and the EL spectra of these copolymers were never contaminated by that green emission band, even after the samples were thermal annealed in air for 2 h (for PL). Furthermore, the EL performance of these copolymers depends on the ratio of the *p*-difluorophenylene units in copolymers. A ratio of 33 mol% of *p*-difluorophenylene units in copolymer led to the highest device current and brightness at a given voltage. The **PF-33F** based OLEDs exhibited a maximum external quantum efficiency of 1.14% (1.14 cd A^{-1}) and the CIE coordinates of (0.16, 0.13), both which were much better than the reference **PFO**.

2. Experimental

2.1. Materials and methods

Chemicals, reagents and solvents from commercial sources are of analytical or spectroscopy grade and used as received without further purification. ^1H NMR spectra were recorded on a Varian INOVA spectrometer (400 MHz). Number-average (M_n) and weight-average (M_w) molecular weights were determined by using a PL-GPC220 instrument with THF as retention solvent and monodisperse polystyrenes (PS) as standards. Elemental analysis was

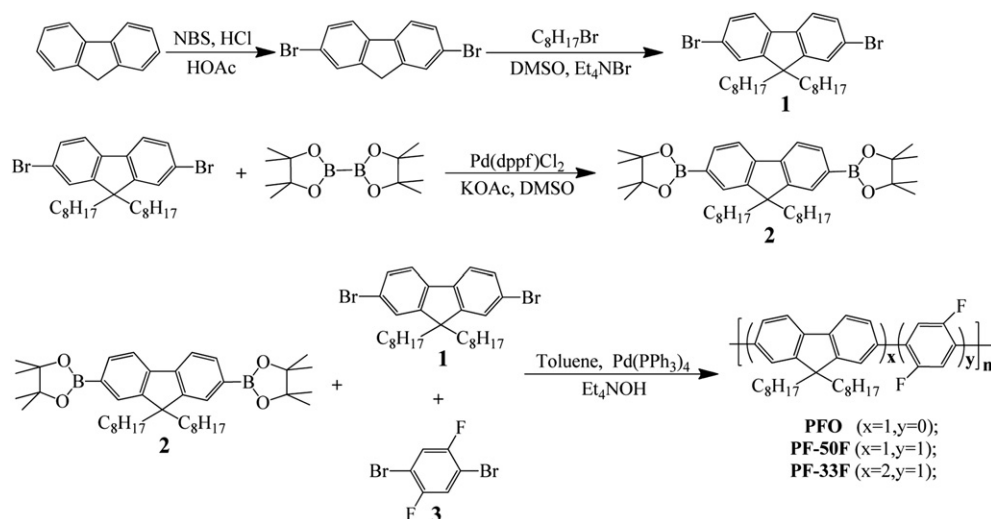
performed on a Carlo–Eriba 1106 elemental analyzer. Thermogravimetry analyses (TGA) and differential scanning calorimetry (DSC) measurements were carried out using a Perkin–Elmer thermogravimeter (Model TGA7) and a Netzsch DSC 204 at a heating rate of $10 \text{ }^\circ\text{C min}^{-1}$ under a nitrogen atmosphere, respectively. The UV–vis absorption and fluorescence spectra measurements were performed on a Perkin–Elmer Lambda 35 UV–Visible spectrophotometer and a Perkin–Elmer LS55 fluorescence spectrometer, respectively. The fluorescence quantum yields were determined against quinine sulfate as the standard ($\Phi = 0.55$, in 0.1 N H_2SO_4). Cyclic voltammetry of the spin-coated films of **PF-33F** on ITO glasses was performed by using a conventional three-electrode configuration and an electrochemical workstation (BAS 100B, USA) at a scan rate of 50 mV s^{-1} . A (0.10 M AgNO_3)/Ag electrode and a platinum wire were used as reference and counter-electrodes. All measurements were made at room temperature in acetonitrile solution, with 0.10 M tetra-*n*-butylammonium hexafluorophosphate (Bu_4NPF_6) as supporting electrolyte.

2.2. Device fabrication and measurements

The pre-cleaned ITO glass substrates ($30 \Omega \square^{-1}$) were treated by UV-Ozone for 20 min. A 40 nm thick PEDOT/PSS film was first spin-coated on pre-treated ITO substrates from aqueous dispersion and baked at $120 \text{ }^\circ\text{C}$ for 40 min in air. Subsequently the polymer solutions (12 mg ml^{-1} in chlorobenzene) were filtered through $0.45 \mu\text{m}$ PTFE filter and spin-coated on PEDOT/PSS film, the thickness of which was controlled as 40 nm by adjusting the spin rate. The substrate was transferred into a vacuum chamber to deposit the TPBI layer at a base pressure less than 10^{-6} torr. Finally, the device fabrication was completed through thermal deposition of LiF (1 nm) and then capping with Al metal (100 nm) as cathode. The emitting area of each pixel is determined by overlapping of two electrodes as 9 mm^2 . The EL spectra, CIE coordinates, and current–voltage–luminance relationships of devices were measured with computer-controlled Spectrascan PR 705 photometer and a Keithley 236 source-measure-unit. All the measurements were carried out in ambient condition at room temperature.

2.3. Synthesis of polymers

The monomers **1** and **2** were synthesized according to the literature method [18], **3** was purchased from Alfa Aesar and used without further purification. The following general procedure was



Scheme 1. Synthetic routes of polymers.

used for the preparation of all the polymers. To a 50 mL two-necked flask were added the appropriate diboronate (1 equiv), the appropriate dibromide (1 equiv), Pd(PPh₃)₄ (0.005 equiv) and toluene (15 mL). The flask equipped with a condenser was then evacuated and filled with argon three times to remove traces of air. The mixture was stirred at 85 °C for 5 min before an aqueous tetraethyl ammonium hydroxide solution (20%, 4.3 equiv) was added. The mixture was then stirred at 85 °C under nitrogen for 24 h. Bromobenzene (1 equiv) was added to the mixture and stirred for 12 h. Phenylboronic acid (1 equiv) was added to the mixture after which the mixture was stirred for 12 h. The mixture was cooled down to room temperature and dropped by pipette into a stirred solution of methanol (100 mL) in a beaker. The precipitate was isolated and extracted with acetone for 12 h in a Soxhlet apparatus, the resulting polymers were collected and dried under reduced pressure.

PFO: Light yellow powder (yield: 81.5%). GPC (THF, PS standard): $M_n = 202,215 \text{ g mol}^{-1}$, $M_w = 269,000 \text{ g mol}^{-1}$, PD = 1.33; ¹H NMR (400 MHz, CDCl₃, TMS): δ 7.84–7.32 (m, ArH), 2.12 (br, CH₂), 1.25–1.15 (m, CH₂), 0.84–0.80 (m, CH₂+CH₃);

PF-50F: White fibrous solid (yield: 93.6%). GPC (THF, PS standard): $M_n = 36,679 \text{ g mol}^{-1}$, $M_w = 59,070 \text{ g mol}^{-1}$, PD = 1.61; ¹H NMR (400 MHz, CDCl₃, TMS): δ 7.87–7.36 (m, ArH), 2.12 (br, CH₂), 1.23–1.13 (m, CH₂), 0.84–0.81 (m, CH₂+CH₃); Elemental analysis found: C 82.48, H 8.40.

PF-33F: White fibrous solid (yield: 93.3%). GPC (THF, PS standard): $M_n = 35,633 \text{ g mol}^{-1}$, $M_w = 54,064 \text{ g mol}^{-1}$, PD = 1.52; ¹H NMR (400 MHz, CDCl₃, TMS): δ 7.87–7.36 (m, ArH), 2.12 (br, CH₂), 1.23–1.12 (m, CH₂), 0.84–0.80 (m, CH₂ + CH₃); Elemental analysis found: C 85.28, H 9.27.

3. Results and discussion

3.1. Synthesis

The general synthetic routes for copolymers **PF-33F** and **PF-50F** and the reference polymer **PFO** are outlined in Scheme 1. They were synthesized by Suzuki polycondensation reaction of monomer **2** (1 equiv.) with **1** and **3** (totally 1 equiv.) in the appropriate molar ratios ([**3**] = 0, **PFO**; [**1**] = 0, **PF-50F**; [**1**]/[**3**] = 0.5, **PF-33F**). The reaction was performed in toluene solution with [Pd(PPh₃)₄] (0.005 equiv.) as catalyst and aqueous tetraethylammonium hydroxide (4.3 equiv) as an emulsifying base. The polymers were end-capped with phenyl groups. Monomers **1** and **2** were synthesized according to literature methods as shown in Scheme 1 [18]. Copolymers **PF-33F** and **PF-50F** were obtained as white fibrous solids in high yields over 90%. They have good solubility in common organic solvents such as tetrahydrofuran, dichloromethane and toluene. The number-average molecular weights (M_n) and weight-average molecular weights (M_w) of these copolymers were determined by gel-permeation chromatography (GPC) using polystyrenes (PS) standards as 35,633 and 54,064 for **PF-33F**, 36,679 and 59,070 for **PF-50F**, respectively. The polydispersity indexes (PDI, $PDI = M_w/M_n$) were calculated as 1.52 and 1.61 for **PF-33F** and **PF-50F**, respectively. A brief summary of these parameters is listed in Table 1.

3.2. Thermal properties

The thermal properties of **PF-33F** and **PF-50F** were investigated by thermogravimetry analysis (TGA) and differential scanning calorimetry (DSC) at a scanning rate of 10 °C min⁻¹ in a nitrogen atmosphere and the results are summarized in Table 1. **PF-33F** and **PF-50F** exhibit high thermal stability with decomposition temperatures (corresponding to 5% weight loss) over 400 °C (see Fig. S1 in the supporting information). Thermally induced phase

Table 1
Structural characterization, thermal and photophysical data of the polymers.

Polymer	Yield (%)	M_n	M_w/M_n	T_g (°C)	$T_{d,5\%}$ (°C)	Φ (%) ^a	$\lambda_{\text{max}}^{\text{abs}}$ (nm) ^b	$\lambda_{\text{max}}^{\text{em}}$ (nm) ^b
PFO	81.5	202,215	1.33	/	/	0.63	387/384	417/432
PF-33F	93.3	35,633	1.52	109	412	0.70	370/370	415/420
PF-50F	93.6	36,679	1.61	n.o. ^c	421	0.73	364/361	403/411

^a Measured in CH₂Cl₂ solution with quinine sulfate as the standard ($\Phi = 0.55$).

^b The data before the slash is for dilute dichloromethane solution, and the data after the slash are for solid films.

^c n.o. = not observed.

transition behaviors of the copolymers were investigated by DSC. As shown by the DSC thermograms in Fig. S2, one endothermic peak due to glass transition was detected at 110 °C (T_g) when a powder of **PF-33F** was heated for the first run. This implies that **PF-33F** was amorphous even when it was directly obtained from organic solvents. When a sample of **PF-50F** was heated, an exothermic peak was observed at 127 °C, which was ascribed to the crystallization. With increasing temperature, the crystal melts at 247 °C. No glass transition was observed for **PF-50F** under the present experimental conditions. The relatively high glass transition temperature for **PF-33F** is an essential merit that is favorable for device stability, especially when it is used under high temperatures [19].

3.3. Photophysical properties

The photophysical properties of these polymers were investigated by means of electronic absorption and photoluminescence (PL) spectra in dilute dichloromethane solutions and solid films on quartz plates. Fig. 1 illustrates the absorption and PL spectra of these polymers in dilute dichloromethane solutions. Similar to the reference **PFO**, the two copolymers exhibit structureless absorption in dilute solutions with peaks at 364 and 370 nm for **PF-50F** and **PF-33F**, respectively, which are ascribed to the π - π^* transition of the polymer backbone. With gradually increasing the ratio of the *p*-difluorophenylene units from **PFO** to **PF-50F**, the absorption spectrum reveals a general trend of a blue shift. The same blue-shift order was observed in the absorption spectra of the polymer films, as shown by the data in Table 1. This is probably because the less coplanarity between the adjacent fluorene and phenylene rings in copolymers than the two fluorenes in **PFO** reduces the conjugation extent in the polymer backbone and thus increases the HOMO–LUMO energy of individual molecules in dilute solution and the energy band gap in solid state. Upon photoexcitation at the absorption maximum, all these polymers emit strong deep blue fluorescence. As shown in Fig. 1b, the fluorescence spectra of these polymers show three well-resolved vibronic bands. For example, the three bands for **PF-33F** are located at 415, 438, and 472 nm, and those for **PFO** are at 417, 440, and 475 nm. The three fluorescence bands of each polymer can be ascribed to the electronic transitions from the lowest vibronic level of the ground state ($S_{0,0}$) to different vibronic levels of the first singlet excited state ($S_{1,0}$, $S_{1,1}$, and $S_{1,2}$). In consistence with the blue shift in absorption spectra, a blue shift is also observed in the PL spectra of these polymers when increasing the ratio of *p*-difluorophenylene units.

From the wavelength difference between the absorption maximum and fluorescence maximum, the Stokes shifts of these copolymers were determined as 45 nm and 39 nm for **PF-33F** and **PF-50F**, respectively, which are both lightly larger than that of **PFO** (30 nm). A larger Stokes shift is usually desired for a light-emitting material since it means a weaker self-absorption and more efficient light output in OLEDs. The fluorescence quantum yields (Φ) of the copolymers were measured in dilute dichloromethane solutions

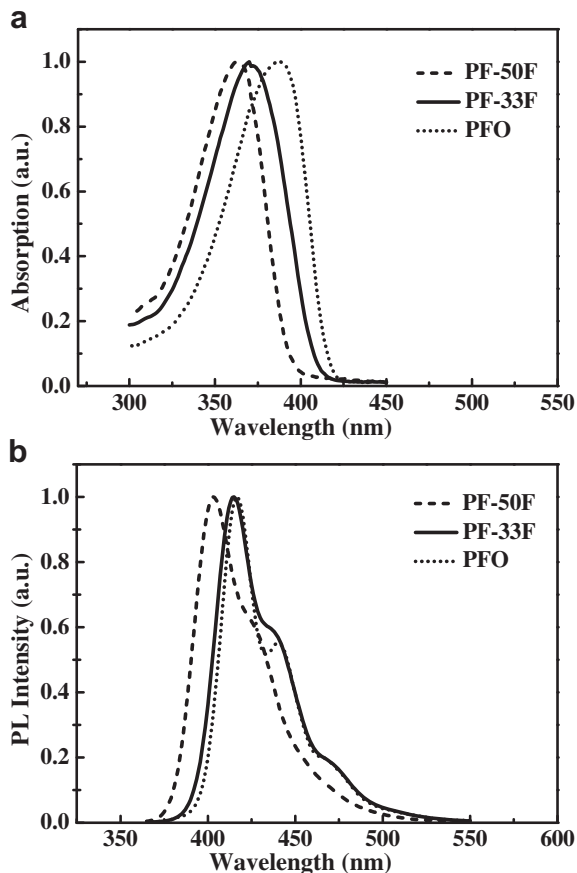


Fig. 1. Absorption a) and fluorescence b) spectra of polymers in dilute dichloromethane solution.

using quinine sulfate ($\Phi = 0.55$ in 0.1 N H_2SO_4) as a reference [20]. They were determined as 0.70 and 0.73 for **PF-33F** and **PF-50F**, respectively, which are both higher than that of **PFO** ($\Phi = 0.63$). There have been similar reports that the introduction of fluorine atoms or trifluoromethyl groups in organic molecules or metal complexes resulted in the increase of the fluorescent or phosphorescent quantum yields [21]. The high fluorescence quantum yields of the present copolymers indicate that they may be promising blue light-emitting materials for application in OLEDs.

3.4. Spectral stability

In order to evaluate the spectral stability of **PF-33F** and **PF-50F**, copolymer films were spin-coated from chlorobenzene solutions onto quartz plates and then thermally annealed in air at various temperatures for 2 h. After the films were cooled to the ambient temperature, PL spectra were measured. **PFO** films were also treated and tested under same conditions for comparison. Fig. 2 shows the fluorescence spectra of these polymer films before and after annealing. It is obvious that the PL spectra of copolymers **PF-33F** and **PF-50F** before and after annealing are almost identical to each other except for the discernable spectral position change that is probably due to physical change or instability of measuring environment [22]. The absence of any new emission band in **PF-33F** and **PF-50F** films excludes the formation of any new emissive species, even after annealing at such a high temperature of 150 °C in air for 2 h. However, under the same conditions, the **PFO** film exhibited the well-known green emission band from 500 to 600 nm after annealing at and over 100 °C. Furthermore, the intensity of the green band became higher with increasing

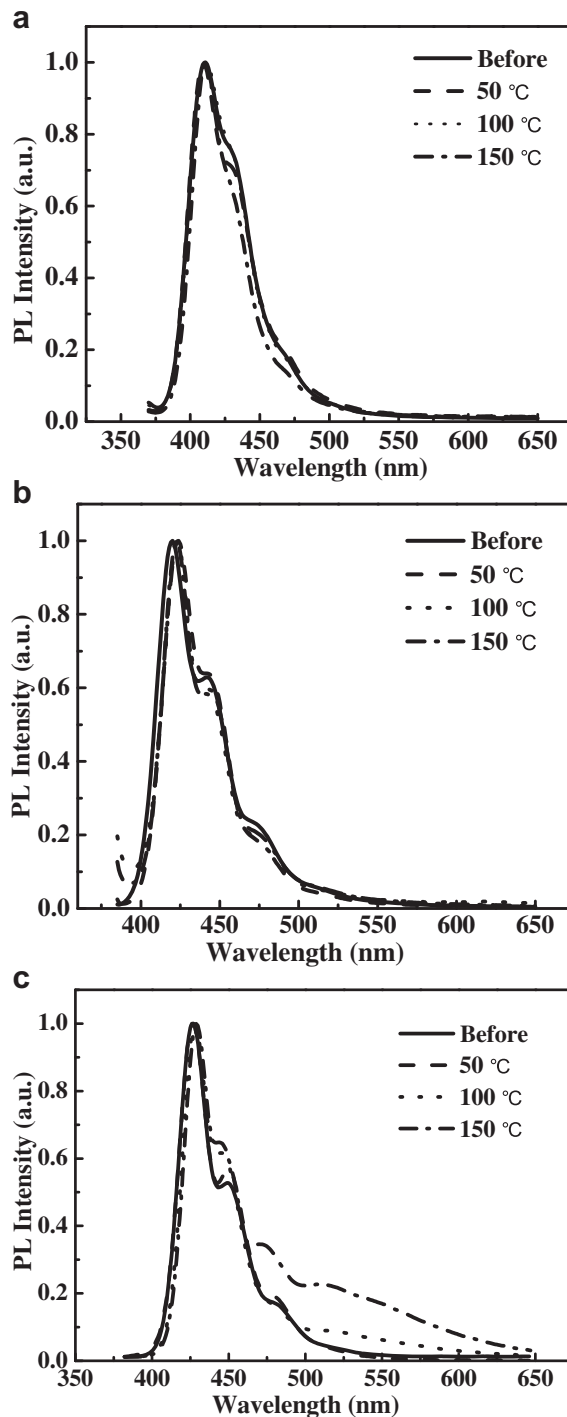


Fig. 2. Fluorescence spectra of a) **PF-50F**, b) **PF-33F** and c) **PFO** films before and after thermal annealing in air at various temperatures.

temperature. It is obvious that the introduction of the *p*-difluorophenylene units to the mainchains in copolymers **PF-33F** and **PF-50F** prevented the formation of the green emission band and improved the color purity and stability of their blue fluorescence.

3.5. Electrochemical properties

In order to investigate the electrochemical properties of the novel copolymers, the **PF-33F** films were made by spin-coating on ITO glass substrates and were used as working electrode in the

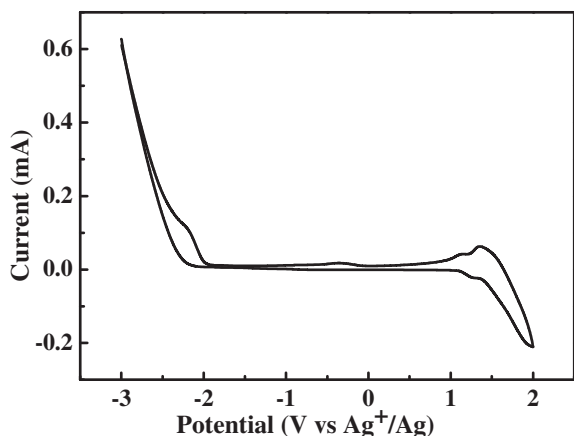


Fig. 3. Cyclic voltammogram of PF-33F film in acetonitrile at a scan rate of 50 mV s⁻¹.

traditional three-electrode set-up. The cyclic voltammogram of PF-33F film is shown in Fig. 3. PF-33F exhibits a reversible one-electron oxidation and irreversible reduction processes. The irreversible reduction was frequently observed for polymers especially when the sample was film [23,24], the real reason of which is still not clear, but may be partially because of the film format. The onset potentials of oxidation and reduction for PF-33F were determined as 1.17 V and -1.95 V versus Ag⁺/Ag. The HOMO and LUMO energy levels were estimated as -5.57 eV and -2.45 eV, respectively, according to the equations of HOMO (eV) = -(E_{ox}^{onset} + 4.4 eV) [25] and LUMO (eV) = -(E_{red}^{onset} + 4.4 eV). The electrochemical bandgap of PF-33F was determined as 3.12 eV by calculating the difference between the onset potentials of oxidation and reduction. Apparently, a HOMO level at -5.57 eV is quite to that of the widely-used hole injecting material PEDOT:PSS (-5.3 eV) and a LUMO level at -2.45 eV is also close to that of the electron-transporting material TPBI (-2.8 eV), implying that efficient hole and electron injections can be expected when PF-33F was used in combination with these functional layers in OLEDs.

3.6. Electroluminescence properties of OLEDs

Based on their pure blue fluorescence and relatively high quantum yields, PF-33F and PF-50F were used as emitting layer to fabricate OLEDs with a configuration of ITO/PEDOT:PSS (40 nm)/polymers (40 nm)/TPBI (20 nm)/LiF (1 nm)/Al (200 nm). The fresh PFO sample was also used to fabricate OLEDs and investigated under

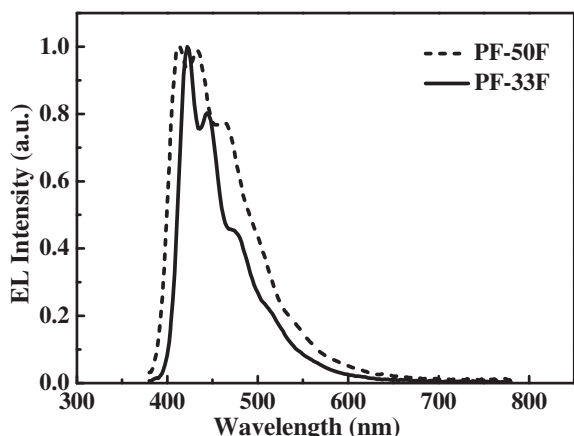


Fig. 4. EL spectra for the PF-33F, and PF-50F based OLEDs.

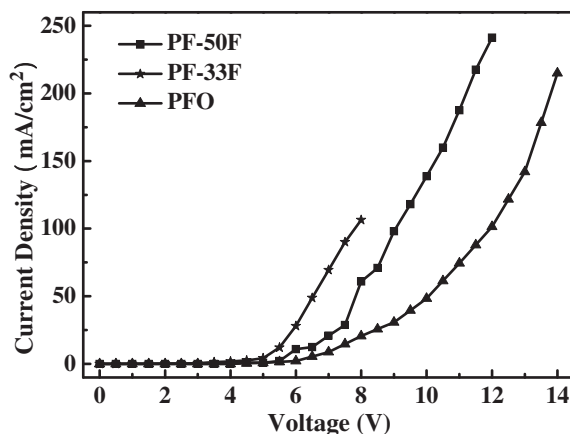


Fig. 5. The current density–voltage characteristics for the PFO, PF-33F, and PF-50F based OLEDs.

identical conditions for comparison. In these devices, PEDOT:PSS acts as hole injection layer (HIL), TPBI as the electron-transporting (ETL) and hole-blocking layer (HBL). The copolymer based devices emitted bright deep-blue light with emission peak at 422 nm and CIE coordinates of (0.16, 0.13) for PF-33F, and 412 nm and CIE coordinates of (0.17, 0.13) for PF-50F, as shown by the EL spectra in Fig. 4. The EL spectra are almost identical in spectral features to their PL of films, except with a slight red-shift of 1–2 nm. The red-shift in EL is a commonly observed phenomena in most organic and polymeric light-emitting diodes, which is probably caused by the influence of the electrical field on the excited states [26]. Moreover, the EL spectra and the CIE coordinates of PF-33F and PF-50F are observed to be insensitive to the driving voltage, indicating a stable blue emission color with respect to the excitation intensity. In contrast, the EL spectra of the PFO device (Figure S3 in the supporting information) always consist of the blue parts at 438, 466 and 494 nm, which correspond to the fine-structured bands in PL of the fresh PFO films, and a broad green component with a peak at 520 nm even at low driving voltage of 5 V. The intensity of the green emission band increased with increasing the driving voltage. It should be noted that the two long-wavelength blue bands also ascended along with the green band. The green emission could be observed in EL of the fresh PFO device, but not in PL of the fresh PF films. There have been similar reports that the green emission from the fluorenone is stronger in EL than in PL [8,27]. This is because the low-energy keto defects can be excited not only by energy transfer from the fluorene

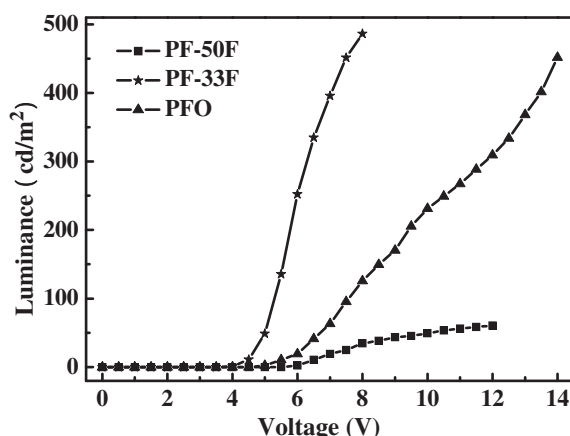


Fig. 6. The luminance–voltage curves for the PFO, PF-33F, and PF-50F based OLEDs.

Table 2
EL performance of the polymers based OLEDs.

Polymer	V_{on} (V) ^a	L (cd m ⁻²) ^b	η_L (cd A ⁻¹) ^b	η_{ext} (%) ^b	λ_{max} (nm)	CIE (x, y)
PFO	4.8	452 (14 V)	0.88 (6 V)	0.53	438	0.18, 0.21
PF-33F	4	486 (8 V)	1.14 (5 V)	1.14	422	0.16, 0.13
PF-50F	5.9	61 (12 V)	0.092 (7 V)	0.086	412	0.17, 0.13

The data in the parentheses are the voltages at which the data are recorded.

^a Turn-on voltage, recorded at 1 cd m⁻².

^b Maximum values of the devices.

moieties but also by direct charge trapping in the EL device made of **PFO**, while only by energy transfer in PL of **PFO** films. Evidently the introduction of the fluorinated moieties in the backbone of these two copolymers also guaranteed the color purity and stability of the EL, which is usually more sensitive to the purity of light-emitting material than PL. It is suggested that the improved spectral purity and stability in both PL and EL of these blue light-emitting copolymers benefit from the presence of *p*-difluorophenylene units which probably take away electron density from the 9-position carbon through π -conjugation channels due to its appropriate electron-withdrawing nature.

The current density–voltage (J – V) characteristics of these OLEDs are illustrated in Fig. 5. In spite of the identical device configuration in the three OLEDs, the **PF-33F** and **PF-50F** based devices exhibited much higher current densities than **PFO** device. It is implied that the introduction of *p*-difluorophenylene units in the copolymer backbone is favorable to increase the charge conductivity of the resultant copolymers. However, when the content ratio of the fluorinated units increased from 33% to 50%, the current density at a given voltage decreased dramatically for **PF-50F** device in comparison to **PF-33F** device. It is proposed that too high ratio of *p*-difluorophenylene units probably act as electron traps and induce unbalance of negative and positive charges.

Fig. 6 shows the luminance–voltage curves for the three OLEDs. All the EL performance data are summarized in Table 2. The **PF-33F** device turned on (to deliver a brightness of 1 cd m⁻²) at a relatively low voltage of 4 V, and reached a maximum luminance of 486 cd m⁻² at 8 V. The luminance at a given voltage decreased dramatically for **PF-50F** device in comparison with the **PF-33F** device despite the slightly higher fluorescent quantum yield for **PF-50F**. This is consistent with the current density trend observed in Fig. 5. A maximum external quantum efficiency of 1.14% (corresponding to a luminance efficiency of 1.14 cd A⁻¹) was achieved for **PF-33F** device at 5 V. Under same experimental conditions, the **PFO** device turned on at a higher voltage of 4.8 V and the maximum external quantum efficiency reached to 0.53% (0.88 cd A⁻¹ at 6 V), which is comparable with the reported data for **PFO** in literatures [11,24]. Evidently, the EL performances of **PF-33F** are much better than the parent **PFO** with improved blue color purity, higher charge mobility, and much higher EL efficiency. This should benefit from the presence of the *p*-difluorophenylene units and its proper content ratio. In addition, the EL efficiency and color coordinates of present copolymers are evidently better than those of most polyfluorene derivatives reported in the literature [11,13,15]. As far as we know, a quantum efficiency of 1.14%, a luminescence efficiency of 1.14 cd A⁻¹ and CIE (0.16, 0.13) achieved for **PF-33F** device are among the best performance reported for blue light-emitting polyfluorenes so far.

4. Conclusion

In summary, two fluorene-based copolymers containing *p*-difluorophenylene units in backbone, **PF-33F** and **PF-50F**, were

synthesized and characterized as deep blue light-emitting materials. The introduction of the fluorinated groups in backbone increased the fluorescent quantum yield and improved the spectra purity and stability. However, 33 mol% of fluorinated units was proved to be the most appropriate ratio leading to satisfied charge mobility. This is one successful example to improve the blue color purity of fluorene-type light-emitting polymers without expense of luminescent quantum yield and charge mobility. A quantum efficiency of 1.14% and CIE (0.16, 0.13) were obtained for **PF-33F** based OLED, among the best performance reported for fluorene-based blue light-emitting polymers so far.

Acknowledgments

We thank the National Natural Science Foundation of China (20923006, and 21072026), the Ministry of Education for the New Century Excellent Talents in University (Grant NCET-08-0074), and the NKBRF (2009CB220009) for financial support of this work.

Appendix A. Supplementary data

Supplementary data associated with this article can be found, in the online version, at doi:10.1016/j.polymer.2012.02.010.

References

- [1] Grimsdale AC, Chan K, Martin RE, Jokisz PG, Holmes AB. Chem Rev 2009;109:897–1091.
- [2] Pogantsch A, Wenzl FP, List EJW, Leising G, Grimsdale AC, Müllen K. Adv Mater 2002;14:1061–4.
- [3] Xiao S, Nguyen M, Gong X, Cao Y, Wu H, Moses D, et al. Adv Funct Mater 2003;13:25–9.
- [4] Scherf U, List EJW. Adv Mater 2002;14:477–87.
- [5] Teetsov JA, Vanden Bout DA. J Am Chem Soc 2001;123:3605–6.
- [6] Montilla F, Mallavia R. Adv Funct Mater 2007;17:71–8.
- [7] Romaner L, Pogantsch A, de Freitas PS, Scherf U, Zojer E, List EJW. Adv Funct Mater 2003;13:597–601.
- [8] Gong X, Iyer PK, Moses D, Bazan GC, Heeger AJ. Adv Funct Mater 2003;13:325–30.
- [9] Cho SY, Grimsdale AC, Jones DJ, Watkins SE, Holmes AB. J Am Chem Soc 2007;129:11910–1.
- [10] Craig MR, de Kok MM, Hofstraat JW, Schenning APHJ, Meijer EW. J Mater Chem 2003;13:2861–2.
- [11] Park SH, Jin YG, Kim JY, Kim SH, Kim JW, Suh HS, et al. Adv Funct Mater 2007;17:3063–8.
- [12] Hung MC, Liao JL, Chen SA, Chen SH, Su AC. J Am Chem Soc 2005;127:14576–7.
- [13] Li JY, Ziegler A, Wegner G. Chem Eur J 2005;11:4450–7.
- [14] Charas A, Morgado J, Marinho JMG, Alcácer L, Lim SF, Friend RH, et al. Polymer 2003;44:1843–50.
- [15] Kamtekar KT, Vaughan HL, Lyons BP, Monkman AP, Pandya SU, Bryce MR. Macromolecules 2010;43:4481–8.
- [16] Kameshima H, Nemoto N, Endo T. J Polym Sci Part A Polym Chem 2001;39:3143–50.
- [17] Assaka AM, Rodrigues PC, de Oliverira ARM, Ding L, Hu B, Karasz FE, et al. Polymer 2004;45:7071–81.
- [18] Jo J, Chi CY, Höger S, Weger G, Yoon DY. Chem Eur J 2004;10:2681–8.
- [19] Ye SH, Liu YQ, Lu K, Wu WP, Du CY, Liu Y, et al. Adv Funct Mater 2010;20:3125–35.
- [20] Ren HC, Li JY, Wang RJ, Zhang T, Gao ZX, Liu D. Polymer 2011;52:3639–46.
- [21] Wang R, Liu D, Ren H, Zhang T, Yin H, Liu G, et al. Adv Mater 2011;23:2823–7.
- [22] Tao S, Peng ZK, Zhang XH, Wang PF, Lee CS, Lee ST. Adv Funct Mater 2005;15:1716–21.
- [23] Zeng DL, Chen JW, Chen Z, Zhu WH, He J, Yu F, et al. Macromol Rapid Commun 2007;28:772–9.
- [24] Yang W, Hou Q, Liu C, Niu Y, Huang J, Yang R, et al. J Mater Chem 2003;13:1351–5.
- [25] Zhang T, Liu D, Wang Q, Wang RJ, Ren HC, Li JY. J Mater Chem 2011;21:12969–76.
- [26] Yamamoto H, Wilkinson J, Long JP, Bussman K, Christodoulides JA, Kafafi ZH. Nano Lett 2005;5:2485–8.
- [27] Lupton JM. Chem Phys Lett 2002;365:366–8.